Int J Adv Manuf Technol (2012) 60:135–147
DOI 10.1007/s00170-011-3576-z

ORIGINAL ARTICLE

Optimization of wire electrical discharge machining process parameters for cutting tungsten

Rong Tai Yang · Chorng Jyh Tzeng · Yung Kuang Yang · Ming Hua Hsieh

Received: 25 March 2011 / Accepted: 7 August 2011 / Published online: 30 August 2011

Abstract This study analyzes variations in metal removal rate (MRR) and quality performance of roughness average (R_a) and corner deviation (CD) depending on parameters of wire electrical discharge machining (WEDM) process in relation to the cutting of pure tungsten profiles. A hybrid method including response surface methodology (RSM) and back-propagation neural network (BPNN) integrated simulated annealing algorithm (SAA) were proposed to determine an optimal parameter setting. The results of 18 experimental runs via a Taguchi orthogonal table were utilized to train the BPNN to predict the MRR, R_a, and CD properties. Simultaneously, RSM and SAA approaches were individually applied to search for an optimal setting. In addition, analysis of variance was implemented to identify significant factors for the processing parameters. Furthermore, the field-emission scanning electron microscope images show that a lot of built-edge layers were presented on the finishing surface after the WEDM process. Finally, the optimized result of BPNN with integrated SAA was compared with that obtained by an RSM approach. Comparisons of the results of the algorithms and confirmation experiments show that both RSM and BPNN/SAA methods are effective tools for the optimization of parameters in WEDM process.

Keywords Optimization · Neural network · Simulated annealing algorithm · Response surface methodology · Wire electrical discharge machining · Pure tungsten

R. T. Yang · C. J. Tzeng · Y. K. Yang (✉) · M. H. Hsieh
Department of Mechanical Engineering,
Minghsin University of Science and Technology,
1, Hsin Hsing Road, Hsin Feng,
304, Hsinchu, Taiwan
e-mail: yky@must.edu.tw

1 Introduction

Wire electrical discharge machining (WEDM) has become an important non-traditional machining process. It is widely used in the aerospace, nuclear, and automotive industries. This is because WEDM provides an effective solution for machining hard materials (like titanium, molybdenum, zirconium, tungsten carbide, etc.) with intricate shapes and profiles that are difficult to machine using conventional methods [1–4]. Cutting velocity and surface roughness are important output parameters. These determine the production efficiency and quality of WEDM [5–8]. In addition, the machining accuracy, especially at corner position, may be destroyed because of some phenomena such as wire defect, vibration, etc. The accuracy of the corner cuts (sharp corners and small fillet radii) may be improved by modifying the cutting parameters and the wire path. Sanchez et al. [9] presented a study on the corner geometry generated by successive cuts (roughing and finishing). Errors at different zones of the corner were identified and related to the material removed during each cut. The influence of limited cutting speed on the accuracy of WEDM corner cutting was then discussed. Han et al. [10] described a simulation method for WEDM in the rough cutting of a corner. In the simulation, they analyzed the vibration of the wire electrode due to the reaction force acting on the wire electrode during the WEDM. They also set up a geometrical model of the wire electrode path and numerical control (NC) path before investigating the relationship between the wire electrode movement and NC movement. Dodun et al. [11] investigated the WEDM corner cutting accuracy. Their experimental work shows that the use of WEDM to obtain outside corners with a small corner angle and small thickness produces a machining error shaped like post-yield bending. Therefore,

improving the production efficiency, quality of surface roughness, and corner cut accuracy of WEDM is a significant area of study. In addition, the selection of optimum cutting parameters is key to obtaining a higher cutting speed or good surface finish. Improperly selected parameters may also result in serious consequences like short-circuiting of the wire and wire breakage. The possibility of wire breakage imposes certain limits on the cutting speed, which in turn reduces productivity. Discharge current, discharge capacitance, pulse duration, pulse frequency, wire speed, wire tension, average working voltage, and dielectric flushing conditions are the machining parameters which affect WEDM performance measures [5–8]. However, the problem of selecting optimum cutting parameters for WEDM processes is not fully solved, even though up-to-date computer numerical control (CNC) WEDM machines are available. Therefore, there is a need to apply a statistical technique to optimize parameters in WEDM processes so as to improve the performance measures.

The Taguchi method has been used quite successfully in several industrial applications to optimize manufacturing processes and in the design of electrical and mechanical components [12–16]. However, Taguchi's method can only find the best set of specified process parameter level combinations which include the discrete setting values of the process parameters. The application of a conventional Taguchi method is unreasonable when the variable of a process parameter is continuous. Response surface methodology (RSM) is also a good method for minimizing the number of experiments to achieve the optimum conditions. Tzeng and Yang [17] implemented RSM to determine the optimal parameters of a CNC turning process for SKD11. Liu et al. [18] used RSM to present the mathematical models for modeling and analysis of the effects of drilling hole in the EDM process parameters, including the discharge current, pulse time on, duty factor, and capacitance value. Chuang et al. [19] applied RSM to determine the optimal parameters of an injection molding process for manufacturing thin-shell plastic parts. Gaitonde et al. [20] also applied RSM to investigate the relationship between cutting conditions and machinability characteristics during the turning processes of metal matrix composites. Recently, back-propagation neural network (BPNN) has become a very powerful and practical method for modeling complex nonlinear systems [21–24]. At the same time, the use of simulated annealing algorithms (SAA) can be found in various research fields for parameter optimization. A means of applying BPNN integrated with SAA has been proposed to improve upon the conventional Taguchi method for optimizing a multiple input–multiple output process parameter design problem. Qiao [25] applied the Davidon–Fletcher–Powell method and SAA approach to optimize a cooling system design in plastic injection molding. Arul et al. [26] applied a SAA approach to search for the optimal process parameters for delamination constrained drilling of glass fiber-reinforced plastics. Sayarshad and Ghoseiri [27] used a SAA approach to optimize a fleet size and freight car allocation problem wherein car demands and travel times were assumed to be deterministic and unmet demands were back-ordered. Yang et al. [28] proposed the optimization methodology of SAA for the selection of the best process parameters for electro-discharge machining. Chen et al. [29] also had conducted BPNN integrated SAA to analyze the variation of cutting velocity and workpiece surface finish that determine an optimal parameter setting of the WEDM process on the manufacture of pure tungsten profiles. The literature [12–29] shows that statistical techniques have, for the most part, been individually applied to the study of optimal process parameters. Therefore, the RSM method and BPNN with integrated SAA approach are used in this paper to model and compare the optimization of WEDM process parameters that affect the metal removal rate (MRR), roughness average (R_a), and corner deviation (CD) on manufactured tungsten profiles.

In this study, analysis of variance (ANOVA) is utilized to examine the most significant factors for the WEDM process parameters. In addition, in order to study the surface texture produced and to identify finishing mechanism, field-emission scanning electron microscope (FE-SEM) images were also examined. Finally, the optimal parameter settings are verified by conducting confirmation experiments and comparing the results of different approaches of RSM and SAA.

2 Experimental setups

2.1 Material

Tungsten exhibits the highest operating temperature of all metals at about 2,900°C (3,173 K) as well as the melting temperature of 3,420°C (3,693 K). By using tungsten powder with a purity of 99.97%, outgassing of impurities can be avoided. This material quality is used for electrodes in high-intensity discharge lamps and, through its high purity, guarantees consistent lamp quality and increased lifetimes [30]. Moreover, the impurities of tungsten can contaminate the environment of semiconductor manufacturing, and a high powder-to-particle ratio will reduce the quality and reliability of semiconductors. Therefore, high-purity tungsten is necessary for semiconductor manufacturing processes. In addition, tungsten has high hardness, toughness, and brittleness and cannot be machined easily. Generally, machining tungsten results in very high tool wear. Robust machine tools and consistent machining conditions are essential, otherwise chips and cracks may occur; therefore, WEDM is a good manufacturing method [30].

Table 1 lists the basic physical properties of the pure tungsten used in the present study, which was provided by PLANSEE Co. [30].

2.2 Schematic of a specimen

Figure 1 shows the machining setup of a WEDM process. The experiments were conducted on a rigid CNC WEDM machine with a maximum output current of 25 A, maximum wire feed rate of 18 m/min, and *x*–*y*-axis feed rate of 0.8 m/min (machine type CW-430F, manufactured by Ching Hung Machinery & Electric Industrial Co., Ltd., Taiwan). A workpiece thickness of 5 mm and a 0.25-mm brass wire (Cu65/Zn35) were used in all the experiments. At the same time, for each set of cutting parameters, continuous cutting with a straight length of 40 mm and orthogonal length of 10 mm was made into the workpiece.

2.3 Experimental design and parameter settings

The product quality produced by WEDM is always affected by process parameters such as the pulse on and off times, peak current, arc on and off times, polarity, servo voltage, no load voltage, duty factor, dielectric constant, feed rate override, wire feed rate, wire tension, water pressure, etc. [5–8]. In this study, experiments were planned using a factorial design based on a Taguchi L_{18} orthogonal array with $2^1 \times 3^6$. Table 2 lists the process factors and factor levels that an experimental factor with two levels (i.e., the pulse on time, factor *A*) and other six experimental factors with three levels include. The pulse on time (i.e., factor *A*), the pulse off time (i.e., factor *B*), arc off time (i.e., factor *C*), the servo voltage (i.e., factor *D*), the wire feed rate (i.e., factor *E*), the wire tension (i.e., factor *F*), and the water pressure (i.e., factor *G*) were the selected factors for the WEDM process. The selection of factors was based on the engineer's experience and the advice from the handbook recommended by the machine manufacturer.

Table 1 Basic physical properties of the pure tungsten

Property	Value
Purity (wt.% tungsten)	99.97%
Melting point	3420°C
Density at 293 K	19.3 g/cm^3
Hardness at 293 K	460 (HV30)
Young's modulus at 293 K (GPa)	396
Poisson's ratio	0.28
electrical conductivity (Ωm)	5.6×10^{-8}
Thermal conductivity at 293 K (W/mK)	138

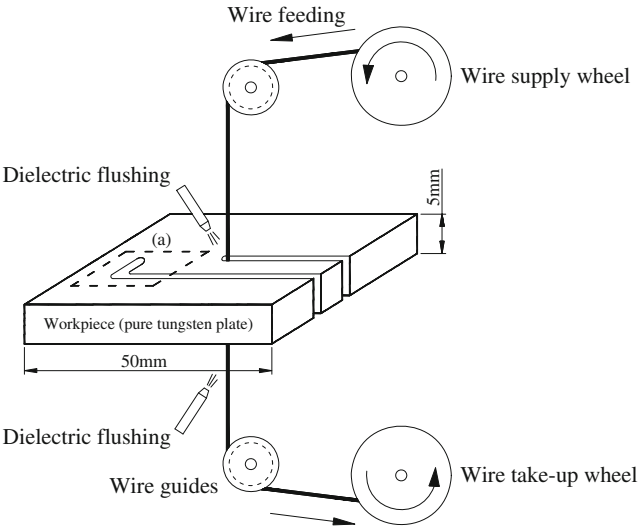

Fig. 1 Scheme of the WEDM process

2.4 Measuring apparatus

2.4.1 Kerf and corner deviation measuring apparatus

The kerf and corner deviation of the workpieces after the WEDM experimental runs were measured using an Optics Zoom Scope (OZS, model no. ZS-3020-VP-MI, Bao-I Tech. Co., Taiwan).

2.4.2 Surface measuring apparatus

The roughness average (R_a) of the surface after WEDM was measured by a surface analyzer (Form Talysurf 50 Taylor Hobson Ltd., UK).

2.4.3 FE-SEM apparatus

The surface texture produced and the finishing mechanism after the WEDM process were observed and investigated using a FE-SEM (JEOL, model no. JSM-6500F, Japan).

Table 2 Process factors and factor levels

Process factors	Level			Unit
	1	2	3	
A: Pulse on time	0.3	0.5	–	μs
B: Pulse off time	12	14	16	μs
C: Arc off time	12	14	16	μs
D: Servo voltage	42	44	46	V
E: Wire feed rate	8.4	9.6	10.8	m/min
F: Wire tension	1,473.33	1,620	1,767.66	gf
G: Water pressure	10.70	12.85	15.00	bar

Fixed parameters: Feed rate override=1.5 rate; Arc on time=0.2 μs

2.5 Experimental results

The kerf is measured using the OZS and is expressed as the sum of the wire diameter and twice the wire–workpiece gap. The kerf value is the average of six measurements made from the workpiece with 2-mm increments along the cut length. MRR is calculated from Eq. 1 [5].

$$\mathrm{MRR} = k \times t \times v_c \times \rho \quad (1)$$

where k is the kerf, t is the thickness of the workpiece (5 mm), v_c is cutting speed (millimeters per minute), and ρ is the density of the workpiece material (19.3 g/cm^3). The cutting speed (v_c) was directly obtained from the computer monitor of WEDM machine.

Corner deviation (CD) was defined as the geometrical contour error on the inner corner by orthogonal cutting. It is denoted and depicted in Fig. 2, which is also the localized enlargement of Fig. 1 (part a). It shows a micrograph of the corner deviation by WEDM operating under the conditions $A_1B_3C_1D_3E_2F_1G_2$ (run no. 9 of Table 3). The measurement data of R_a and CD, v_c, kerf, and the calculated results of MRR were listed in Table 3.

3 Optimization methodologies and results

The optimization methodologies used include RSM, neural networks, and optimization algorithms necessary for developing the proposed approach. Figure 3 illustrates the flowchart used to find an optimal setting for the WEDM process. The following sections detail each of the steps.

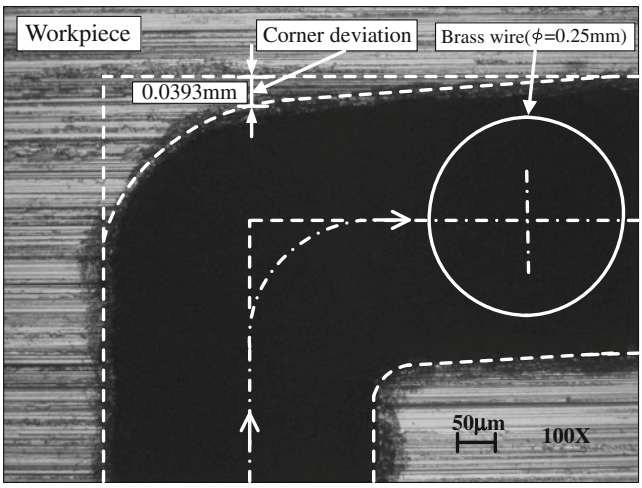

Fig. 2 Localized enlargement of Fig. 1, part (*a*). Corner deviation by a WEDM operation under the conditions $A_1B_3C_1D_3E_2F_1G_2$ (run no. 9 of Table 3)

Step 1 Identify the objectives of the problem: This study aimed to identify an optimal setting to minimize the R_a and CD as well as maximize the MRR.

Step 2 Propose experiments: Use an orthogonal array table to design and conduct the experiments.

Step 3 Experiment and measurement: The experiments were carried out on a rigid CNC wire electrical discharge machine. The MRR, R_a, and CD were measured.

Step 4 Analysis of variance: ANOVA was applied to identify the most significant factors.

Step 5 Optimization process: RSM and BPNN/SAA approaches were used to obtain an optimal setting.

Step 6 Compare results: The results were compared with those predicted through modeling. Optimal settings determined by RSM and BPNN/SAA were also compared.

3.1 Analysis of variance

In order to analyze the results of the experimental designs, ANOVA is utilized. ANOVA is used to investigate the relationship between a response variable and one or more independent variables. It can be determined whether the difference between the average of the levels is greater than what could reasonably be expected from the variation that occurs within the level. A "model F value" is calculated from a model mean square divided by a residual mean square. It is a test of comparing a model variance with a residual variance. If the variances are close to being the same, the ratio will be close to 1 and it is less likely that any of the factors have a significant effect on the response. As for a "model P value," if the "model P value" is very small (<0.05), then the terms in the model have a significant effect on the response [31]. Similarly, an "F value" on any individual factor terms is calculated from a term mean square divided by a residual mean square. It is a test that compares a term variance with a residual variance. If the variances are close to being the same, the ratio will be close to 1 and it is less likely that the term has a significant effect on the response. Furthermore, if a "P value" of any model terms is very small (<0.05), the individual terms in the model have a significant effect on the response. The results of ANOVA are shown in Table 4.

Table 4 lists the ANOVA result of the MRR. The contribution percentages for the MRR are 70.66% and 13.04% by the factor terms "A" (the pulse on time) and "B" (the pulse off time), respectively. The other factor terms can be regarded as insignificant due to their smaller "contribution percentage" compare with the factor terms "A" and "B".

Table 4 also lists the ANOVA results of the R_a. The contribution percentages for R_a are 84.88% and 7.91% by

Table 3 Results of experimental runs

Run no.	*A*	*B*	*C*	*D*	*E*	*F*	*G*	Data		Result		
								v_c (mm/min)	Kerf (mm)	MRR (g/min)	R_a (μm)	CD (mm)
1	1	1	1	1	1	1	1	7.4074	0.339	0.2423	1.1786	0.0378
2	1	2	2	2	2	2	2	6.7567	0.334	0.2178	1.3362	0.0366
3	1	3	3	3	3	3	3	6.4102	0.337	0.2085	1.4561	0.0306
4	1	1	1	2	2	3	3	7.5987	0.329	0.2412	1.2691	0.0295
5	1	2	2	3	3	1	1	6.4516	0.335	0.2086	1.2369	0.0389
6	1	3	3	1	1	2	2	6.5359	0.336	0.2119	1.3362	0.0349
7	1	1	2	1	3	2	3	7.5019	0.332	0.2403	1.4023	0.0373
8	1	2	3	2	1	3	1	6.5359	0.332	0.2094	1.3049	0.0291
9	1	3	1	3	2	1	2	6.1881	0.340	0.2030	1.2786	0.0393
10	2	1	3	3	2	2	1	7.7942	0.348	0.2617	1.6453	0.0328
11	2	2	1	1	3	3	2	9.3809	0.346	0.3082	1.8159	0.0273
12	2	3	2	2	1	1	3	7.5988	0.350	0.2566	1.9534	0.037
13	2	1	2	3	1	3	2	8.5763	0.344	0.2845	1.6711	0.0255
14	2	2	3	1	2	1	3	8.3333	0.346	0.2786	1.7254	0.0371
15	2	3	1	2	3	2	1	7.4074	0.349	0.2493	1.6653	0.0315
16	2	1	3	2	3	1	2	8.1103	0.349	0.2733	1.8234	0.0368
17	2	2	1	3	1	2	3	8.0000	0.349	0.2697	1.8414	0.0295
18	2	3	2	1	2	3	1	7.6923	0.343	0.2548	1.6273	0.0243

the factor terms "*A*" (the pulse on time) and "*G*" (the water pressure), respectively. Again, the other factor terms can be regarded as insignificant due to their smaller "contribution percentage" compare with the factor terms "*A*" and "*G*".

Table 4 also lists the ANOVA results of the CD. The contribution percentages for CD are 14.70% and 78.10% by the factor terms "*A*" (the pulse on time) and "*F*" (the wire tension), respectively. Yet again, the other factor terms can be regarded as insignificant due to their smaller "contribution percentage" compared with the factor terms "*A*" and "*F*".

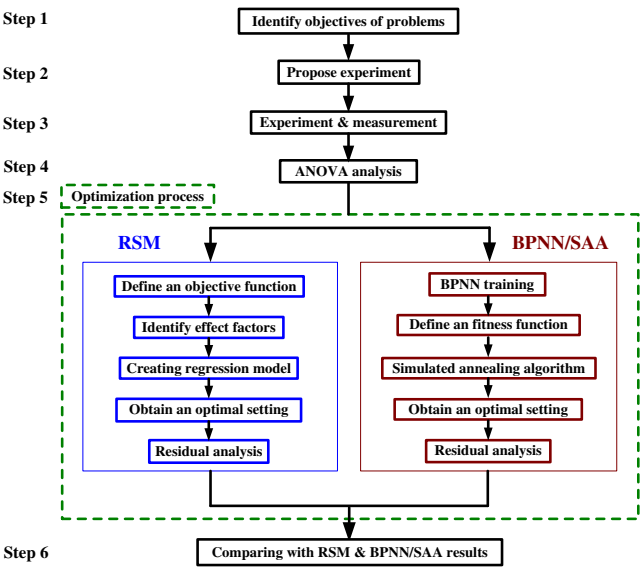

Fig. 3 Flowchart of the optimization process

3.2 Response surface methodology

RSM is a statistical technique for determining and representing the cause and effect relationship between true mean responses and input control variables. The main idea of RSM is to use a set of designed experiments to obtain an optimal response. In this work, response surface modeling is utilized for determining the relations between the various WEDM process parameters with the various machining criteria and for exploring the effect of these process parameters on the responses, i.e., the MRR, R_a, and CD. In the general case, the response surface is described by an equation of the form [31]:

$$Y = \beta_0 + \sum_{i=1}^{n} \beta_i x_i + \sum_{i=1}^{n} \beta_{ii} x_i^2 + \sum_{j=2}^{n} \sum_{i=1}^{j-1} \beta_{ij} x_i x_j \ldots \quad (2)$$

where Y is the corresponding response, e.g., the MRR, R_a, and CD produced by the various process variables of WEDM; the x_i (1, 2,…, n) are coded levels of n quantitative process variables; and the terms β_0, β_i, β_{ii}, and β_{ij} are the second-order regression coefficients. The second term under the summation sign of this polynomial equation is

Table 4 ANOVA of MRR, R_a, and CD

Source	Analysis of MRR						Analysis of R_a						Analysis of CD					
	Sum of squares	Degree of freedom	Mean square	*F* value	*P* value	Contribution (%)	Sum of squares	Degree of freedom	Mean square	*F* value	*P* value	Contribution (%)	Sum of squares	Degree of freedom	Mean square	*F* value	*P* value	Contribution (%)
Model	1.54E−02	7	2.20E−03	26.99	<0.0001	94.97	9.72E−01	7	1.39E	23.50	<0.0001	94.27	3.78E	7	5.39E	37.76	<0.0001	96.35
A	1.14E−02	1	1.14E−02	140.56	<0.0001	70.66	8.75E−01	1	8.75E	148.12	<0.0001	84.88	5.76E	1	5.76E	40.32	<0.0001	14.70
B	2.11E−03	1	2.11E−03	25.95	0.0005	13.04	8.92E−03	1	8.92E	1.51	0.2475	0.86	3.67E	1	3.67E	0.26	0.6230	0.09
C	4.14E−04	1	4.14E−04	5.09	0.0477	2.56	4.90E−03	1	4.90E	0.83	0.3841	0.47	3.41E	1	3.41E	2.39	0.1532	0.87
D	8.37E−04	1	8.37E−04	10.28	0.0094	5.17	1.59E−04	1	1.59E	0.03	0.8729	0.02	3.67E	1	3.67E	0.26	0.6230	0.09
E	1.57E−05	1	1.57E−05	0.19	0.6694	0.10	1.09E−03	1	1.09E	0.18	0.6769	0.11	6.16E	1	6.16E	4.31	0.0645	1.57
F	1.63E−04	1	1.63E−04	2.00	0.1878	1.00	2.24E−04	1	2.24E	0.04	0.8494	0.02	3.06E	1	3.06E	214.22	<0.0001	78.10
G	3.95E−04	1	3.95E−04	4.85	0.0523	2.44	8.16E−02	1	8.16E	13.80	0.0040	7.91	3.63E	1	3.63E	2.54	0.1420	0.93
Residual	8.14E−04	10	8.14E−05	–	–	5.03	5.91E−02	10	5.91E	–	–	5.73	1.43E	10	1.43E	–	–	3.65
Cor total	1.62E−02	17	–	–	–	100.00	1.03E+00	17	–	–	–	100.00	3.92E	17	–	–	–	100.00

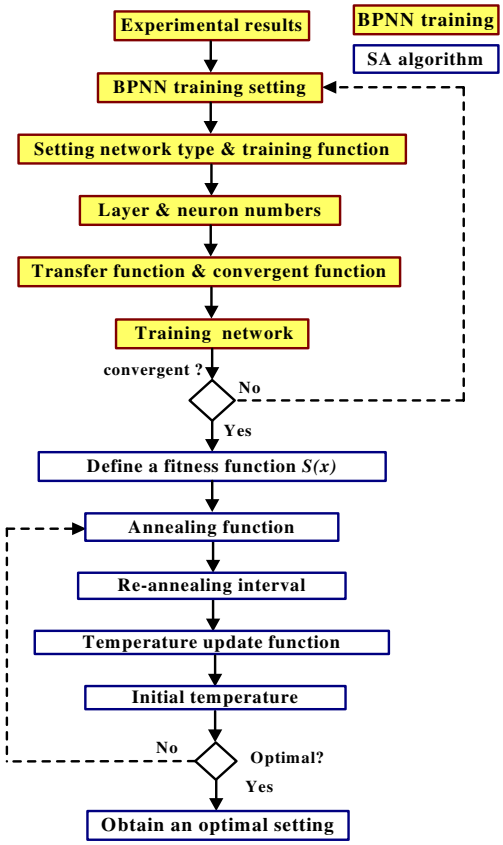

Fig. 4 Flowchart of the BPNN integrated SAA math specimen

attributable to the linear effect, whereas the third term corresponds to the higher-order effects; the fourth term of the equation includes the interactive effects of the process parameters.

The objective of this study was to identify an optimal setting for process parameters that can minimize the measured R_a and CD as well as maximize the MRR of a

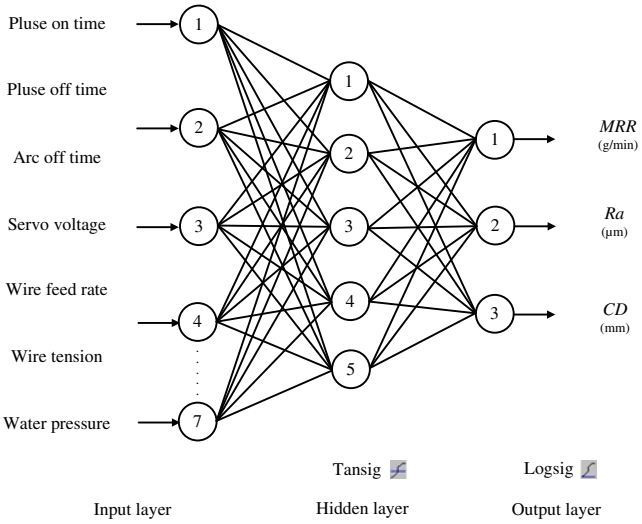

Fig. 5 Architecture of the BPNN model for the WEDM process

WEDM process. Therefore, the objective function, $F(x)$, can be defined as follows:

$$d_1 = \left[\frac{\mathrm{MRR}_i - \mathrm{MRR}_{\min}}{\mathrm{MRR}_{\max} - \mathrm{MRR}_{\min}}\right] \tag{3}$$

$$d_2 = \left[\frac{Ra_{\max} - Ra_i}{Ra_{\max} - Ra_{\min}}\right] \tag{4}$$

$$d_3 = \left[\frac{\mathrm{CD}_{\max} - \mathrm{CD}_i}{\mathrm{CD}_{\max} - \mathrm{CD}_{\min}}\right] \tag{5}$$

$$\begin{aligned} \mathrm{DF} &= \left(d_1^{w_1} \times d_2^{w_2} \times d_3^{w_3}\right)^{1/(w_1+w_2+w_3)} \\ F(x) &= -\mathrm{DF} \end{aligned} \tag{6}$$

where w_1, w_2, and w_3 are the weightings of importance for MRR, R_a, and CD, respectively. $\mathrm{MRR}_{\max}$ and $\mathrm{MRR}_{\min}$ are the maximum and minimum values of MRR. Similarly, $R_{a\,\max}$ and $R_{a\,\min}$, and $\mathrm{CD}_{\max}$ and $\mathrm{CD}_{\min}$ are the maximum and minimum values of R_a and CD, respectively. The values of w_1, w_2, and w_3 are identical since MRR, R_a, and CD are equally important in this study. DF is a desirability function [31]; the objective is to choose an optimal setting to maximize the desirability function, DF, i.e., minimize $F(x)$.

3.2.1 Development of mathematical predictive models

A combined desirability function can be calculated from Eq. 6. At the same time, by considering the insignificant terms via ANOVA—the "P value" of any model term is >0.05—the individual terms in the model have an insignificant effect on the response [31]. Namely, the insignificant terms of the machining parameters can be removed without reducing the operation performance of the regression models. In addition, the experimental analysis and developed regression models in this paper were performed using the Design Expert version 6.0.10 software (Stat-Ease, Inc.). In this work, Eq. 2 can be rewritten according to the result of the software run. Mathematical predictive models for the MRR, R_a, and CD are shown as follows:

$$\begin{aligned} \mathrm{MRR} = {} & 4.2814 \times 10^{-1} + \left(2.5208 \times 10^{-1} \times A\right) \\ & - \left(6.6326 \times 10^{-3} \times B\right) \\ & - \left(2.9374 \times 10^{-3} \times C\right) \\ & - \left(4.1755 \times 10^{-3} \times D\right) \\ & + \left(2.6672 \times 10^{-3} \times G\right) \end{aligned} \tag{7}$$

$$R_a = 1.5660 \times 10^{-1} + (2.2053 \times A) + \left(3.8348 \times 10^{-2} \times G\right) \quad (8)$$

$$\mathrm{CD} = 9.5863 \times 10^{-2} - \left(1.7888 \times 10^{-2} \times A\right) - \left(3.4315 \times 10^{-5} \times F\right) \quad (9)$$

3.2.2 Optimal setting through the use of RSM

An optimal setting can be obtained through RSM by choosing appropriate combinations of WEDM process parameters as starting values. This optimal setting gives an appropriate combination of pulse on time of 0.43 μs, pulse off time of 12.00 μs, arc off time of 12.00 μs, servo voltage of 42.00 V, wire feed rate of 10.48 m/mim, wire tension of 1,764.43 gf, and water pressure of 10.71 bar.

3.3 BPNN integrating SAA

Figure 4 shows the flowchart used to find an optimal process through BPNN with integrated SAA. At the same time, the Matlab Neural Network Toolbox was used as a platform to create the networks.

3.3.1 BPNN training

A BPNN is usually divided into three parts: the input layer, the hidden layer, and the output layer. The information contained in the input layer is mapped to the output layers through the hidden layers. Each unit can only send its output to the units on the higher layer and receive its input from the lower layer. More hidden layers can be added to obtain a powerful multilayer network. The architecture of the BPNN model used in this study for the WEDM process is shown in Fig. 5. The node number of the hidden layer was determined by train trials, and the final value obtained was 5, which made the configuration of BPNN 7–5–3. A hyperbolic tangent-sigmoid transfer function was used as the activation function for the hidden layers, and a log-sigmoid transfer function was used for the output layers. Simultaneously, the Levenberg–Marquardt reduction scheme was also selected for the neural network algorithm. The convergent function is as follows:

$$\mathrm{MSE} = \frac{1}{N}\sum_{i=1}^{N}(d_i - y_i)^2$$

where N is the experimental time, d_i is the experimental value, and y_i is the predicted value of the neural network for training sample i.

In this study, the Matlab Neural Network Toolbox was used as a platform to create the networks. The BPNN training process settled that an appropriate combination of conditions was 1,000 for the number of iterations, 0.001 for performance goal, 5 for maximum validation failure number, 10^{-10} for minimum performance gradient, and 25 for epochs between displays.

3.3.2 SAA optimization

Various numerical optimization algorithms have been developed to solve optimization problems. Unfortunately, no universal algorithm exists which works well for all problems. This is because the convergence and the efficiency of a particular algorithm are dependent on the problem to be solved. In this study, the optimal WEDM process parameters for cutting pure tungsten profiles was identified using the SAA as follows.

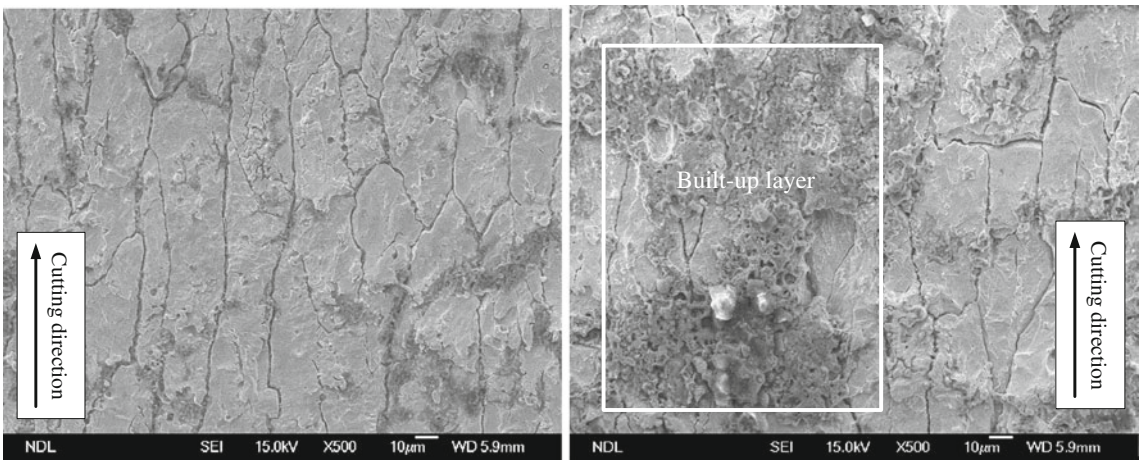

Fig. 6 **a** FE-SEM micrograph on the surface finish of after a WEDM operation under the conditions $A_1B_1C_1D_1E_1F_1G_1$ (run no. 1 of Table 3). **b** FE-SEM micrograph on the surface finish of after a WEDM operation under the conditions $A_2B_2C_1D_1E_3F_3G_2$ (run no. 11 of Table 3)

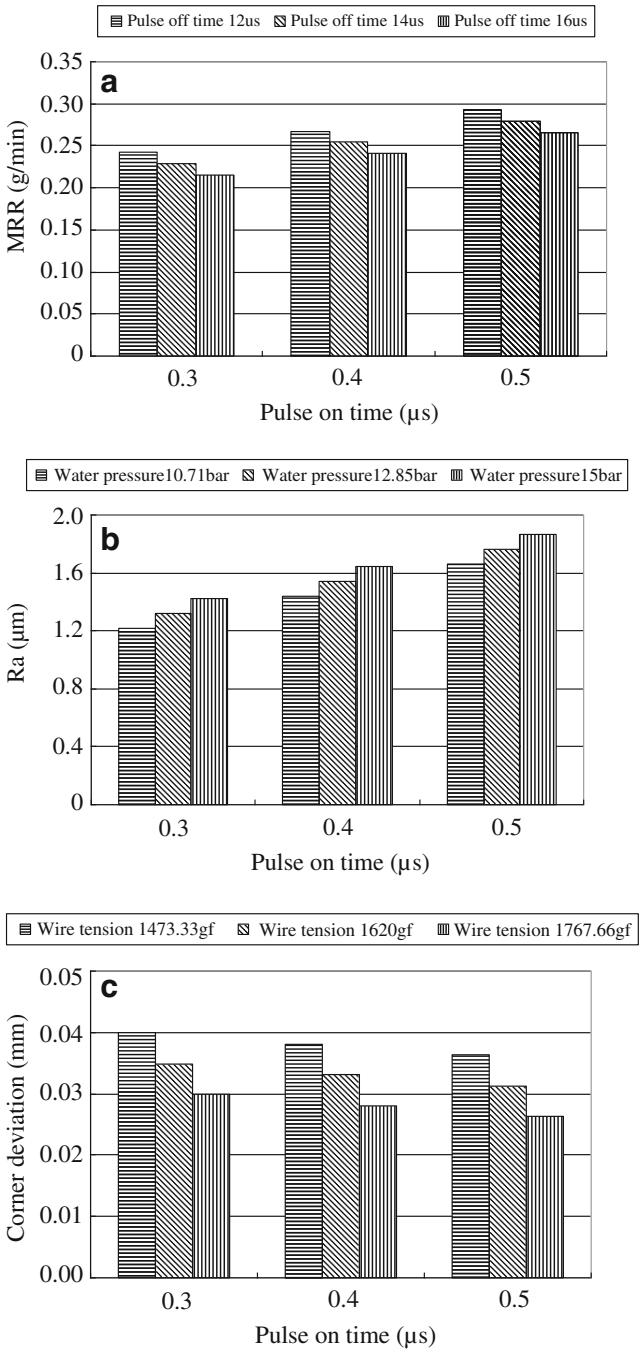

Fig. 7 **a** Variation of MRR with pulse on time/pulse off time different cutting conditions. **b** Variation of R_a with pulse on time/water pressure different cutting conditions. **c** Variation of *CD* with wire tension/pulse on time different cutting conditions

Define a fitness function S(x) The formulation of $S(x)$ for using in SAA search approach can be defined as follows:

$$\text{Minimize } S(x) = \sum_{i=1}^{k} \left(y_{ti} - y_{pi}\right)^2$$

$$\text{Subject to } \mathrm{LCL}_i \leqq y_{pi} \leqq \mathrm{UCL}_i$$

$$\mathrm{LCL} = \mu - n\varepsilon;\ n = 1, 2, \ldots, N$$

$$\mathrm{UCL} = \mu + n\varepsilon;\ n = 1, 2, \ldots, N$$

x	process parameters
k	total number of response which is nominal-the-best type and has a certain target
y_t	predicted value of i response that is a nominal-the-best type response
y_p	certain target value
UCL_i	upper control limit of i response
LCL_i	lower control limit of i response
μ	mean value of experimental data
ε	standard deviation of experimental data

Annealing approach Annealing function selects Boltzmann annealing which takes random steps, with a size proportional to the square root of temperature.

Reannealing interval We set the reannealing interval to be 100; this is the number of points to accept before reannealing.

Temperature updates function Exponential temperature update decreases as $0.95^{\text{iteration}}$.

Initial temperature Initial temperature is the temperature at the beginning of the run; it was set to 100°C for all experiments, namely, a relatively faster convergence can be obtained using initial temperature 100°C.

3.3.3 Optimal setting of BPNN/SAA approaches

An optimal setting was obtained by choosing appropriate combinations of WEDM process parameters via a BPNN/SAA approach. An appropriate combination was calculated to be: pulse on time of 0.43 μs, pulse off time of 12.84 μs, arc off time of 12.73 μs, servo voltage of 42.41 V, wire feed rate of 8.89 m/min, wire tension of 1,693.64 gf, and water pressure of 10.74 bar.

4 Results and discussions

4.1 Observation of the cutting surface

Figure 6a, b shows the FE-SEM micrographs in which the surface finish of the specimens after the WEDM operations can be examined. Figure 6a displays the surface finish after cutting using parameters $A_1B_1C_1D_1E_1F_1G_1$ (i.e., run no. 1 of Table 3). Some fine cracks parallel to the direction of the cutting were found. At the same time, Fig. 6b displays the surfaces finish obtained under the cutting conditions of $A_2B_2C_1D_1E_3F_3G_2$ (i.e., run no. 11 of Table 3). At the same time, it can be seen from Fig. 6b that a lot of built-edge layers were presented. Figure 6b shows that the higher

Table 5 Residual results of MRR, R_a, and CD using RSM and BPNN

Run no.	Results using RSM									Results using BPNN								
	MRR (g/min)			R_a (μm)			CD (mm)			MRR (g/min)			R_a (μm)			CD (mm)		
	Actual	Pred.	Residual	Actual	Pred.	Residual	Actual	Pred.	Residual	Actual	Pred.	Residual	Actual	Pred.	Residual	Actual	Pred.	Residual
1	0.2423	0.2421	0.0002	1.1786	1.2285	−0.0499	0.0378	0.0399	−0.0021	0.2423	0.2425	−0.0002	1.1786	1.1836	−0.0050	0.0378	0.0390	−0.0012
2	0.2178	0.2203	−0.0026	1.3362	1.3110	0.0252	0.0366	0.0349	0.0017	0.2178	0.2064	0.0113	1.3362	1.2897	0.0465	0.0366	0.0364	0.0002
3	0.2085	0.1986	0.0099	1.4561	1.3934	0.0627	0.0306	0.0298	0.0008	0.2085	0.2093	−0.0008	1.4561	1.4610	−0.0049	0.0306	0.0308	−0.0002
4	0.2412	0.2452	−0.0040	1.2691	1.3934	−0.1243	0.0295	0.0298	−0.0003	0.2412	0.2415	−0.0003	1.2691	1.2815	−0.0124	0.0295	0.0295	0.0000
5	0.2086	0.2063	0.0023	1.2369	1.2285	0.0084	0.0389	0.0399	−0.0010	0.2086	0.2058	0.0027	1.2369	1.2468	−0.0099	0.0389	0.0393	−0.0004
6	0.2119	0.2096	0.0024	1.3362	1.3110	0.0252	0.0349	0.0349	0.0000	0.2119	0.2083	0.0036	1.3362	1.3421	−0.0059	0.0349	0.0349	0.0000
7	0.2403	0.2477	−0.0073	1.4023	1.3934	0.0089	0.0373	0.0349	0.0024	0.2403	0.2415	−0.0011	1.4023	1.4030	−0.0007	0.0373	0.0373	0.0000
8	0.2094	0.2087	0.0007	1.3049	1.2285	0.0764	0.0291	0.0298	−0.0007	0.2094	0.2111	−0.0017	1.3049	1.3040	0.0009	0.0291	0.0290	0.0001
9	0.2030	0.2046	−0.0016	1.2786	1.3110	−0.0324	0.0393	0.0399	−0.0006	0.2030	0.2051	−0.0021	1.2786	1.2864	−0.0078	0.0393	0.0393	0.0000
10	0.2617	0.2641	−0.0023	1.6453	1.6696	−0.0243	0.0328	0.0313	0.0015	0.2617	0.2613	0.0004	1.6453	1.6547	−0.0094	0.0328	0.0328	0.0000
11	0.3082	0.2850	0.0232	1.8159	1.7521	0.0638	0.0273	0.0263	0.0010	0.3082	0.3027	0.0055	1.8159	1.8135	0.0024	0.0273	0.0272	0.0001
12	0.2566	0.2632	−0.0066	1.9534	1.8345	0.1189	0.0370	0.0364	0.0006	0.2566	0.2568	−0.0001	1.9534	1.9045	0.0489	0.0370	0.0370	0.0000
13	0.2845	0.2757	0.0088	1.6711	1.7521	−0.0810	0.0255	0.0263	−0.0008	0.2845	0.2842	0.0003	1.6711	1.6615	0.0096	0.0255	0.0253	0.0002
14	0.2786	0.2790	−0.0004	1.7254	1.8345	−0.1091	0.0371	0.0364	0.0007	0.2786	0.2758	0.0028	1.7254	1.7915	−0.0661	0.0371	0.0370	0.0001
15	0.2493	0.2576	−0.0083	1.6653	1.6696	−0.0043	0.0315	0.0313	0.0002	0.2493	0.2509	−0.0015	1.6653	1.6616	0.0037	0.0315	0.0315	0.0000
16	0.2733	0.2781	−0.0048	1.8234	1.7521	0.0713	0.0368	0.0364	0.0004	0.2733	0.2761	−0.0028	1.8234	1.7641	0.0593	0.0368	0.0369	−0.0001
17	0.2697	0.2740	−0.0043	1.8414	1.8345	0.0069	0.0295	0.0313	−0.0018	0.2697	0.2702	−0.0005	1.8414	1.8634	−0.0220	0.0295	0.0295	0.0000
18	0.2548	0.2601	−0.0053	1.6273	1.6696	−0.0423	0.0243	0.0263	−0.0020	0.2548	0.2552	−0.0003	1.6273	1.6384	−0.0111	0.0243	0.0249	−0.0006
Averaged error (%)			2.15			3.40			3.24			0.89			1.12			0.54

Table 6 Confirmation runs of MRR, R_a and *CD* by two different approaches

Applied method	Optimal parameters							MRR (g/min)	R_a (μm)	CD (mm)
	A (μs)	*B* (μs)	*C* (μs)	*D* (V)	*E* (m/min)	*F* (gf)	*G* (bar)	Pred./Exp.	Pred./Exp.	Pred./Exp.
RSM	0.43	12.00	12.00	42.00	10.48	1,764.43	10.71	0.2754/0.2801	1.5200/1.4745	0.0276/0.0285
BPNN/SAA	0.43	12.84	12.73	42.41	8.89	1,693.64	10.74	0.2994/0.2925	1.2843/1.3125	0.0262/0.0274

pulse on time, the more intense the discharge energy becomes and the more powerful is the explosion, which can increase the metal removal rate and also results in brass wire of cutting tool accelerating depletion; the residual particle of brass wire was adhered on the cutting surface. This will generate a larger built-up layer and therefore produces rougher surfaces.

4.2 Influence of cutting conditions on the MRR, R_a, and CD

Figure 7a–c shows the significant factor of cutting condition that can be implemented based on the results of ANOVA and BPNN/SAA for the MRR, R_a, and CD. Figure 7a shows the variations of MRR under cutting conditions with different pulse on times and pulse off times. The results of the BPNN/SAA approach suggested that an appropriate combination of parameters was 12.73 μs of arc off time, 42.41 V of servo voltage, 8.89 m/min of wire feed rate, 1,693.64 gf of wire tension, and 10.74 bar of water pressure. Figure 7a indicates that MRR increases with an increase in the pulse on time when a similar pulse off time is used. The higher the discharge energy produced by an increase of the pulse on time, the more powerful is the explosion, and this enables an increased MRR. Similarly, MRR decreases with an increased pulse off time for a constant pulse on time.

Figure 7b shows the variations of R_a with various pulse on times and water pressures when other cutting conditions were set to 12.84 μs of pulse off time, 12.73 μs of arc off time, 42.41 V of servo voltage, 8.89 m/min of wire feed rate, and 1,693.64 gf of wire tension. Figure 7b plots the main effects; as pulse on time increased, the surface roughness of the machined surface increased. This is because the discharge energy becomes more intense with increased pulse on times; the more powerful is the explosion, the MRR is increased (as shown in Fig. 7a) and the brass wire of cutting tool accelerates depletion, which leads to generate the built-up layer. With increased built-up layer, this results in a rougher surface. Hence, to obtain a smooth surface finish for a WEDM workpiece, pulse on time should be set as low as possible. Figure 7b also shows that with the pulse on time held constant, increasing the water pressure results in a slightly increased R_a.

Figure 7c shows the BPNN estimate for the CD with variable pulse on time and wire tension when using constant pulse off time of 12.84 μs, arc off time of 12.73 μs, servo voltage of 42.41 V, wire feed rate of 8.89 m/min, and water pressure of 10.74 bar. Figure 7c clearly indicates that CD decreases with an increase in wire tension with a constant pulse on time, which illustrates that a higher wire tension has resulted in stronger forces acting on the wire, responsible for wire deformation decreases that withstand a component of force with corner cutting, and therefore CD can be reduced. Moreover, CD also decreases with an increase in the pulse on time when wire tension is held constant.

4.3 Comparison of results from different approaches

4.3.1 Residual analysis

In order to check prediction errors of the RSM analysis and BPNN training results, the residual results, which are defined as the differences between the actual and predicted values for each point in the design, can be calculated.

Table 5 lists the residuals based on the RSM approach. The percentage errors for MRR, R_a, and CD are 2.15%, 3.40%, and 3.24%, respectively. Table 5 also shows the residuals based on the BPNN training results. The percentage errors for MRR, R_a, and CD, are 0.89%, 1.12%, and 0.54%, respectively. By comparison, the percentage errors for MRR, R_a, and CD via a trained BPNN are less than those measured from regression models derived by the RSM approach.

4.3.2 Confirmation experiment runs

The data from the confirmation experiment runs and their comparison to the predicted values for MRR, R_a, and CD are listed in Table 6.

The first predicted run of Table 6 shows that an RSM approach gives optimal parameters of pulse on time 0.43 μs, pulse off time 12.00 μs, arc off time 12.00 μs, servo voltage 42.00 V, wire feed rate 10.48 m/min, wire tension 1,764.43 gf, and a water pressure of 10.71 bar. The values predicted by the regression models for the MRR, R_a, and CD are 0.2754 g/min, 1.5200 μm, and 0.0276 mm, respectively. At the same time, with this combination of

parameters, the confirmation runs show MRR, R_a, and CD to be 0.2801 g/min,1.4745 μm, and 0.0285 mm, respectively. Furthermore, for the second predicted run, which is also an optimal run found by the BPNN/SAA method, the parameters were set at: pulse on time, 0.43 μs; pulse off time, 12.84 μs; arc off time, 12.73 μs; servo voltage, 42.41 V; wire feed rate, 8.89 m/min; wire tension, 1,693.64 gf; and water pressure, 10.74 bar. With these parameters, the proposed algorithm predicts the MRR, R_a, and CD to be 0.2994 g/min, 1.2843 μm, and 0.0262 mm, respectively. Confirmation experiments show that the MRR, R_a, and CD are 0.2925 g/min, 1.3125 μm, and 0.0274 mm, respectively. By comparison, the BPNN/SAA approach produced better predictions of the confirmation results than the RSM method.

5 Conclusions

This research proposes an effective process parameter optimization approach that integrates Taguchi's parameter design method, response surface methodology (RSM), back-propagation neural network (BPNN), and simulated annealing algorithm (SAA) on WEDM processes. The proposed approach can effectively assist engineers in determining the optimal process parameter settings for the WEDM process under multi-response consideration. According to the implementation, the results obtained in the illustrative example are summarized as follows:

1. With the higher pulse on time, which leads to the discharge energy becoming more intense, the metal removal rate was increased and the brass wire of cutting tool accelerates depletion, generates a larger built-up layer, and therefore produces rougher surfaces. Simultaneously, increasing the wire tension results in the decrease of corner deviation (CD).
2. This modeling approach was validated through two additional sets of experimental data in order to verify the quality of the algorithm. By comparison, the percentages of residual via a trained BPNN are less than those predictions from the regression models derived by the RSM approach. At the same time, the BPNN/SAA approach produced better quality than the RSM method for the confirmation results of the optimization process parameters.
3. The modeling and optimization methods proposed in this paper show great potential in complicated industrial applications. Obviously, this confirms the excellent reproducibility of the experimental conclusions. Moreover, the results have been successfully applied to a production line manufacturing semiconductor components operated by Chin Shun Precision Industry Co., Taiwan.

Acknowledgment The authors would like to thank the National Science Council of the Republic of China for financially supporting this research (contract no. NSC 97-2221-E-159-006) and Ming-Hsin University of Science and Technology (contract no. MUST-97-ME-009).

References

1. Sarkar S, Sekh M, Mitra S, Bhattacharyya B (2008) Modeling and optimization of wire electrical discharge machining of γ-TiAl in trim cutting operation. J Mater Process Technol 205(1–3):376–387
2. Bamberg E, Rakwal D (2008) Experimental investigation of wire electrical discharge machining of gallium-doped germanium. J Mater Process Technol 197(1–3):419–427
3. Rakwal D, Bamberg E (2009) Slicing, cleaning and kerf analysis of germanium wafers machined by wire electrical discharge machining. Mater Manuf Process 209(8):3740–3751
4. Garg RK, Singh KK, Sachdeva A, Sharma VS, Ojha K, Singh S (2010) Review of research work in sinking EDM and WEDM on metal matrix composite materials. Int J Adv Manuf Technol 50(5–8):611–624
5. Mahapatra SS, Patnaik A (2007) Optimization of wire electrical discharge machining (WEDM) process parameters using Taguchi method. Int J Adv Manuf Technol 34(9–10):911–925
6. Prasad DVSSSV, Gopala Krishna A (2009) Empirical modeling and optimization of wire electrical discharge machining. Int J Adv Manuf Technol 43(9–10):914–925
7. Rao RV, Pawar PJ (2009) Modelling and optimization of process parameters of wire electrical discharge machining. Proc IME B J Eng Manuf 223(11):1431–1440
8. Gauri SK, Chakraborty S (2010) A study on the performance of some multi-response optimisation methods for WEDM processes. Int J Adv Manuf Technol 49(1–4):155–166
9. Sanchez JA, Rodil JL, Herrero A, Lacalle LNL, Lamikiz A (2007) On the influence of cutting speed limitation on the accuracy of wire-EDM corner-cutting. J Mater Process Technol 182(1–3):574–579
10. Han F, Zhang J, Soichiro I (2007) Corner error simulation of rough cutting in wire EDM. Preci Eng 31(4):331–336
11. Dodun O, Gonçalves-Coelho AM, Slătineanu L, Nagîţ G (2009) Using wire electrical discharge machining for improved corner cutting accuracy of thin parts. Int J Adv Manuf Technol 41(9–10):858–864
12. Yang YK, Chang TC (2006) Experimental analysis and optimization of a photo resist coating process for photolithography in wafer fabrication. Microelectronics J 37(8):746–751
13. Yang YK, Shie JR, Liao HT, Wen JL, Yang RT (2008) A study of Taguchi and design of experiments method in injection molding process for polypropylene components. J Reinf Plast Comp 27 (8):819–834
14. Kurt M, Bagci E, Kaynak Y (2009) Application of Taguchi methods in the optimization of cutting parameters for surface finish and hole diameter accuracy in dry drilling processes. Int J Adv Manuf Technol 40(5–6):458–469
15. Badkar DS, Pandey KS, Buvanashekaran G (2011) Parameter optimization of laser transformation hardening by using Taguchi method and utility concept. Int J Adv Manuf Technol 52(9–12):1067–1077
16. Sushil K, Satsangi PS, Prajapati DR (2010) Optimization of green sand casting process parameters of a foundry by using Taguchi's method. Int J Adv Manuf Technol 55:23–34. doi:10.1007/s00170-010-3029-0
17. Tzeng CJ, Yang YK (2008) Determination of optimal parameters for SKD11 CNC turning process. Mater Manuf Process 23(4):363–368
18. Liu NM, Chiang KT, Horng JT, Chen CC (2010) Modeling and analysis of the edge disintegration in the EDM drilling cobalt-bonded tungsten carbide. Int J Adv Manuf Technol 51(5–8):587–598

19. Chuang MT, Yang YK, Hsiao YH (2009) Modeling and optimization of injection molding process parameters for thin-shell plastic parts. Polymer Plast Tech Eng 48(7):745–753
20. Gaitonde VN, Karnik SR, Paulo Davim J (2009) Some studies in metal matrix composites machining using response surface methodology. J Reinf Plast Compos 28(20):2445–2457
21. Karunakar DB, Datta GL (2008) Prevention of defects in castings using back propagation neural networks. Int J Adv Manuf Technol 39(11–12):1111–1124
22. Vafaeesefat A (2009) Optimum creep feed grinding process conditions for Rene 80 super alloy using neural network. Int J Precis Eng Manuf 10(3):5–11
23. Öktem H (2009) An integrated study of surface roughness for modelling and optimization of cutting parameters during end milling operation. Int J Adv Manuf Technol 43(9–41):852–861
24. Zemin F, Jianhua M (2011) Back prediction of high-strength sheet metal under air bending forming and tool design based on GA–BPNN. Int J Adv Manuf Technol 53(5–8):473–483
25. Qiao H (2006) A systematic computer-aided approach to cooling system optimal design in plastic injection molding. Int J Mech Sci 48(4):430–439
26. Arul S, Samuel Raj D, Vijayaraghavan L, Malhotra SK, Krishnamurthy R (2006) Modeling and optimization of process parameters for defect toleranced drilling of GFRP composites. Mater Manuf Process 21(4):357–365
27. Sayarshad HR, Ghoseiri K (2009) A simulated annealing approach for the multi-periodic rail-car fleet sizing problem. Comput Oper Res 36(6):1789–1799
28. Yang SH, Srinivas J, Mohan S, Lee DM, Balaji S (2009) Optimization of electric discharge machining using simulated annealing. J Mater Process Technol 209(9):4471–4475
29. Chen HC, Lin JC, Yang YK, Tsai CH (2010) Optimization of wire electrical discharge machining for pure tungsten using a neural network integrated simulated annealing approach. Exp Syst Appl 37(10):7147–7153
30. PLANSEE high performance materials. www.plansee.com/
31. Montgomery DC (2005) Design and analysis of experiment, 6th edn. Wiley, New York